FINAL REPORT FOR

PHYSICS OF DEBRIS CLOUDS FROM HYPERVELOCITY IMPACTS

NASA-39131-DO#9

4/10/1992 to 10/9/1993

Submitted to
NASA
Marshall Space Flight Center, AL 35812

by

Ralph Zee
Principal Investigator
Materials Engineering Program
Auburn University, AL 36849

Tel: (205) 844-3320
Fax: (205) 844-3400
email: rzee@eng.auburn.edu

FINAL REPORT FOR

PHYSICS OF DEBRIS CLOUDS FROM HYPERVELOCITY IMPACTS

NASA-39131-DO#9

4/10/1992 to 10/9/1993

Submitted to
NASA
Marshall Space Flight Center, AL 35812

by

Ralph Zee
Principal Investigator
Materials Engineering Program
Auburn University, AL 36849

Tel: (205) 844-3320
Fax: (205) 844-3400
email: rzee@eng.auburn.edu

PHYSICS OF DEBRIS CLOUDS FROM HYPERVELOCITY IMPACTS

NASA-NAS8-39131-DO9, Duration: 4/10/92 - 10/9/93

Final Report Submitted to

NASA

Marshall Space Flight Center, AL 35812

Ralph Zee, Principal Investigator

Table of Contents

PHYSICS OF DEBRIS CLOUDS FROM HYPERVELOCITY IMPACTS

NASA-NAS8-39131-DO9, Duration: 4/10/92 - 10/9/93

Final Report Submitted to
NASA
Marshall Space Flight Center, AL 35812

Ralph Zee, Principal Investigator
Materials Engineering Program, Auburn University, AL 36849
Tel: (205) 844-3320, Fax: (205) 844-3400, email: rzee@eng.auburn.edu

I. ABSTRACT OF INVESTIGATION

The protection scheme developed for long duration space platforms relies primarily upon placing thin metal plates or "bumpers" around flight critical components. The effectiveness of this system is highly dependent upon its ability to break up and redistribute the momentum of any particle which might otherwise strike the outer surface of the space craft. Therefore it is of critical importance to design the bumpers such that maximum dispersion of momentum is achieved. This report is devoted to an in-depth study into the design and development of a laboratory instrument which would permit the in-situ monitoring of the momentum distribution as the impact event occurs. A series of four designs were developed, constructed and tested culminating with the working instrument which is currently in use. Each design was individually tested using the Space Environmental Effects Facility (SEEF) at the Marshall Space Flight Center in Huntsville, Alabama. Along with the development of the device, an experimental procedure was developed to assist in the investigation of various bumper materials and designs at the SEEF. Preliminary results were used to compute data

which otherwise were not experimentally obtainable. These results were shown to be in relative agreement with previously obtained values derived through other methods. The results of this investigation indicated that momentum distribution could in fact be measured in-situ as the impact event occurred thus giving a more accurate determination of the effects of experimental parameters on the momentum spread. Data produced by the instrument indicated a Gaussian-type momentum distribution.

A second apparatus was developed and it was placed before the shield in the line of travel utilized a plate to collect impact debris scattered backwards. This plate had a passage hole in the center to allow the particle to travel through it and impact the proposed shield material. Applying the law of conservation of angular momentum a backward momentum vector was determined from the angular velocity of the plate. The forward scattered and backward scattered momentum values were then analyzed to judge the distribution of debris. Loss of momentum was attributed to the inaccuracies of the means of measurement. Assumptions of symmetrical debris for the forward and backward scattered directions also contributed to this loss.

II. INTRODUCTION

The recent development and impending deployment of the Space Station Freedom has led to a resurgence in interest to develop methods for protecting long duration space platforms from the threat of orbiting debris[1,2]. This debris is present in large quantities primarily in the regions of space adjacent to the earth known as the low earth orbits (LEO)[3-5]. This large population of debris can be attributed to the extensive use of this region by space ventures spanning the last forty years[6,7]. The debris is present in both natural forms (micrometeroids) as well as man-made (solid rocket motor exhaust, paint chips, metallic remnants of exploded satellites, etc.)[8-12]. The velocities of these particles range from a few kilometers per second to as high as seventy kilometers per second. While most forms of natural debris are transient in these regions, the man-made form is usually not.[13] It is this threat of collision with hypervelocity debris that jeopardizes any long duration mission in the LEO region of space[14-16]. This problem has become so immense that many countries have developed space debris policies[17,18]. The policies will attempt to regulate the production of any future debris[19-25]. With a designed lifetime of thirty years, the Space Station Freedom will be a likely candidate to experience a collision with debris[26]. It is therefore of utmost concern to designers of this and other future space endeavors that a reliable and cost effective system be developed to protect the platform from catastrophic damage by these collisions.

In 1947, Whipple hypothesized the existence of orbiting debris and its' potential threat to spacecraft[27]. He proposed at that time to shield critical components of spacecraft with thin metal plates known as "bumpers". These bumpers would serve to intercept an incident particle, disintegrate it, and redistribute its momentum over a larger area. This concept has

been researched extensively throughout the past[28-31]. It was employed as a means to protect previous long duration space systems such as Skylab[32]. The requirements drawn up for Space Station Freedom will be the most demanding ever, due in part to its size and duration of occupancy. Thus, a well researched and carefully developed design criteria for the bumper system must be developed.

The process of properly designing a micrometeroid/debris (m/d) protection system involves the determination of certain parameters such as bumper composition (material), thickness, and orientation upon the production and behavior of the debris cloud[33-39]. One such method for establishing these relationships is through the use of computer simulations known as hydrocodes. These programs model the interactions which take place between the impacting particle and the bumper shield. Hydrocodes are a particular type of numerical analysis programs designed specifically to investigate the interactions which take place between solid objects and fluids[40]. Due to the extremely high velocities involved in m/d impacts, the behavior of the projectile with respect to the target is better represented by a solid striking a semi-fluid. Through the use of high speed computers, it is possible to predict the response of an orbiting debris particle striking a bumper. Nevertheless there are certain intrinsic limitations involved in the numerical modeling of hypervelocity impacts. To begin with, debris cloud composition is often a mixture of three different phases of the projectile and bumper matter. This creates a difficult situation for accurately modeling these interactions. In addition, there are limitations in the computing resources available for solving the large quantities of equations associated with hydrocode models. Although computers are becoming more powerful both in terms of speed and capacity, the time

increment for which the hydrocode model is solved can quickly exceed even the best computer systems. This can, of course, result in excessive operating costs. It is for this reason that researchers must make many assumptions in order to simplify the models and cut the solution time down to a more reasonable duration. These assumptions add an inherent degree of uncertainty to any model and therefore limit the ability to accurately describe the debris cloud's characteristics. The other method for determining the effects of bumper designs upon debris cloud formation is through direct laboratory simulation and experimentation.

The experimental determination of debris cloud characteristics such as momentum distribution, requires the use of several unique technologies including the light gas gun (LGG), ultra high-speed photography, and specialized laboratory instrumentation such as the Forward Scatter Momentum Monitoring Device (FSMMD). One of the obvious limitations to simulating hypervelocity impacts is achieving orbital velocities within the laboratory environment. This also includes the containment of the post impact debris which is accompanied by high heat and pressure produced by the collision. This makes it more difficult to design a device capable of withstanding such a harsh environment. Perhaps the most utilized method of experimental analysis is the post event inspection of the debris cloud or an object which has "witnessed" this debris[41]. Figure 1 illustrates the typical setup used for this type of data gathering. In some instances trapping mediums are employed such as styrofoam or low density gels to actually catch the debris cloud fragments after they have been formed[42]. With this method it is possible to trace the individual particles path and combine this with mass data to determine the velocity and momentum. The drawbacks to

this method are the complicated and time consuming setup which must precede each experiment, and the fact that the debris cloud does not necessarily consist solely of solid particles. Thus the damage caused by liquid, or more importantly, vapor phases can not be easily accounted for. Therefore, this method would not be considered as an effective laboratory system for measuring debris momentum distributions. The witness plate technique is, however, a much simpler and easily implemented method for analyzing the effects of bumper parameters upon debris clouds. In this case, the debris cloud is allowed to strike a second plate which is itself robust enough to prevent puncture. The individual particles in the cloud produce craters in the plate which can be analyzed for determining particle velocity, mass, and composition. Unfortunately, this method does not permit an in-situ monitoring of momentum within the debris cloud and only provides a total net effect approach towards cloud momentum analysis. This is not to say that the witness plate technique does not have significant capacity for providing researchers with basic ballistic limit data in an easy to set-up arrangement. For this reason, it exists as the most utilized method in existence for analyzing effects of bumper configurations upon debris clouds. Since neither the trapping medium nor the witness plate methods are capable of providing momentum distributions of the debris cloud in a quantitative manner, it is evident from these analysis methods that the requirements for any device which will monitor debris cloud momentum distributions must be as follows:

1. Provide accurate quantitative values of momentum at selected locations within the debris cloud,
2. Require short turn-around times between each use,

3. Must be easy to obtain results quickly (Provide the possibility of observing the debris cloud momentum instantaneously),
4. Must survive repeated uses in the LGG environment between retrofits,
5. Must be economically beneficial.

These requirements serve as the basis for the efforts put forth in this thesis. The FSMMD was developed with the primary intention of providing useful information quickly and accurately for use in debris shield design criteria determination.

The development of a back scattered momentum monitoring device(BSMMD) and the refinement of the forward scattered momentum monitoring device(FSMMD) were necessary to find high repeatability momentum multiplication values. The existing forward scattered momentum monitoring device was to be improved by providing additional data points further characterizing the forward scattered or upstream debris cloud. The development of a backward scattered device was to show the amount of debris that will be sprayed in the direction opposite to initial particle travel, or downstream. The final designs for each are included in this report to assist any parties interested in pursuing this method of measurement in determination of high velocity and hypervelocity impact damage.

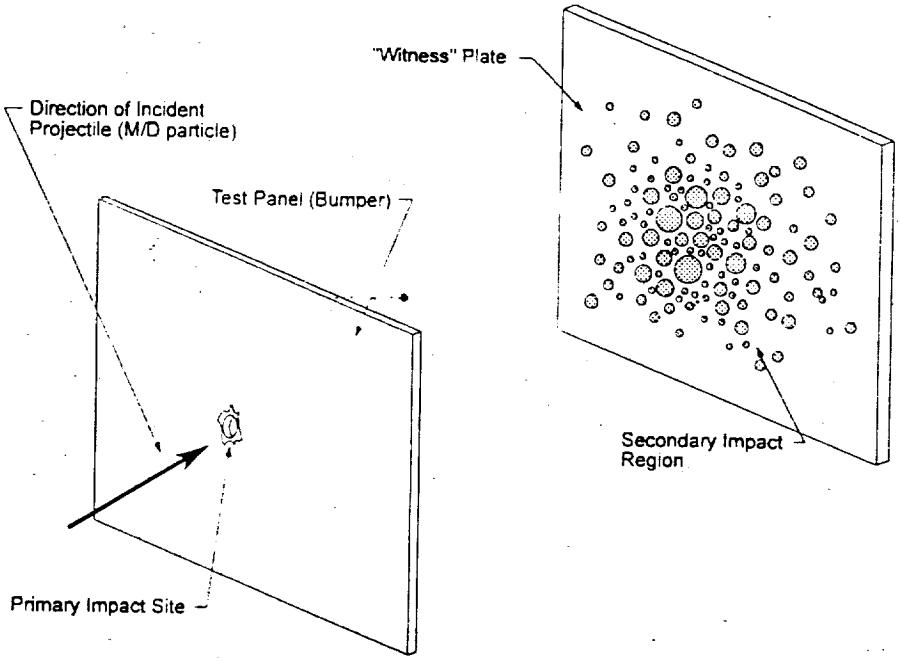

Figure 1. Witness Plate Technique

III. LITERATURE SUMMARY

III.1. Hypervelocity Impact Research

One of the methods currently employed by researchers for determining the effectiveness of proposed bumper systems, is the post-event examination of the bumper plate itself and an additional plate, referred to as the "witness", which catches the resulting debris. While this approach permits testing of many possible combinations of bumper thicknesses, materials, and locations, it does not permit a detailed analysis of what the debris cloud is composed of (distribution of mass) and how it changes with these different configurations. However, other methods do exist by which it is possible to characterize the debris cloud more accurately.

One such method is the high speed flash camera. Using a sophisticated and complex timing system, it is possible to actually photograph the debris cloud as it is forming and eventually colliding with the witness plate. This information allows one to specifically isolate and track individual particles of solid or liquid matter as they travel inside the debris cloud. With this capability, it is possible to determine exact velocities and estimate mass distributions within the cloud. The limitations to the flash camera technique are attributed to the fact that typical illumination sources utilize x-rays and thus require that the projectiles and bumpers be metallic. Recent efforts in this field have included the use of laser holography to capture debris cloud images[43]. Even with these new capabilities, researchers are still hindered by the inability to measure the momentum of the debris cloud directly in part due to the complexity of these systems. This leads to further examination of alternative methods for observing debris cloud momentum distribution.

One such alternative available to researchers is the ballistic pendulum. The ballistic pendulum typically consists of a thick plate suspended by a support apparatus which restricts movement to the direction parallel to the incident projectile. The plate is then positioned inside the test chamber behind the bumper plate and in essence takes the place of the witness panel. After the primary impact between the projectile and the bumper has occurred, the resulting debris cloud then strikes the pendulum assembly producing a corresponding motion. This motion can then be recorded and the total effective momentum of the debris cloud can be extracted. Several researchers have employed this technique with varying degrees of success. In work conducted by the Air Force, researchers employed two separate techniques for monitoring debris cloud momentum distributions. The first method, which was designed to measure localized momentum at certain locations throughout the cloud, consisted of a series of blocks or flyer plates arranged on a horizontal flat surface. The debris cloud was allowed to impact these blocks sending them on various paths at different velocities. These movements were recorded using a pulsed x-ray source coupled with film located under the blocks. The results of this experiment indicated the momentum imparted by the debris cloud to the individual flyer plates from the velocities and masses involved. The other method employed by this study consisted of a flat plate suspended by cables which was free to move only in the direction parallel to the incident projectile. After the debris cloud's formation, a large portion of it was blocked by a second plate containing a small aperture which permitted only a small degree of the cloud to proceed through and strike the pendulum plate. Figure 2 illustrates the typical configuration of the ballistic pendula used in these studies. The movement of these pendula were then recorded by cameras which picked up reflected light

from a mirror placed near the end of the pendulum. By utilizing this arrangement, it became possible to obtain the total debris momentum resolved in the direction of the incident projectile. This technique was also employed by the Southwest Research Institute (S_wRI) in their attempt to obtain momentum values for determining impact phenomenon at extremely high velocities[44]. The difficult nature of these techniques coupled with the harsh environment inside the test chamber prompted the abandonment in most of these attempts to determine momentum distribution. Thus the motivation behind this thesis has evolved from the necessity to accomplish these goals.

Previous methods for monitoring momentum in debris clouds have relied primarily upon the use of the ballistic pendulum. Several researchers have attempted to design systems by which momentum can be measured during or after the actual impact event. Most of these were concerned primarily with obtaining a net integrated momentum value and not with a momentum profile. In only one case has the author found any attempt made towards devising a method for determining momentum distribution. It should be noted that much of the research conducted regarding hypervelocity impact is classified and therefore cannot be reported on.

It appears that the primary motivation for determining momentum values within debris clouds was to help provide empirical values for equations being developed regarding hypervelocity impact studies. These equations were being developed to describe in what fashion momentum was being transferred from an impacting particle to the surface it was striking. In 1964, Denardo and Nysmith, conducted experiments at the NASA Ames Research Center regarding this phenomenon[45]. They were interested in developing a

technique for monitoring the momentum transferred by an orbiting debris fragment to a momentum sensitive sensor which would in turn allow the monitoring of a given orbit for debris population and size distribution. In their study, 2017-T4 Al spheres were fired into target plates composed of 2024-T4 and 1100-0 Al. Their method for monitoring momentum relied upon the transfer of the particle's momentum to the target plate, which was suspended allowing for free movement along the axial direction. By monitoring the pendulum's movement they were able to calculate the momentum imparted by the projectile onto the target plate. Later research conducted in 1968 by Denardo and Nysmith involved the attempt to monitor the momentum transferred from an impacting particle to a second target which represented a spacecraft hull after striking the primary target[46]. This research was aimed at developing a method for obtaining an optimized bumper hull design for future spacecraft. Unlike their previous study, the investigators attempted to monitor the momentum of the actual debris cloud after the primary impact. Like the previous investigation, the impacting particle was represented by an aluminum sphere, and the bumper and hull were represented by thin aluminum plates. The ballistic pendula used in this study were attached to both the primary target or bumper and also to two polyethylene catcher plates. It should be noted that the researchers in this study considered measuring the debris cloud momentum to be excessively difficult and therefore attempted only to measure the ejecta or backscattered debris momentum. The values for the forwardscattered or debris cloud momentum were therefore calculated from the projectile, target, and ejecta momentum by the following equation [1]:

$$mv = (MV)_T + (MV)_S - (MV)_E \qquad [1]$$

where mv represented the incident projectile momentum, $(MV)_T$ the target momentum, $(MV)_S$ spray or debris cloud momentum, and $(MV)_E$ the ejecta momentum.

In the previously mentioned studies conducted by S_wRI in 1989, researchers Mullins, et al attempted to devise a method for directly measuring the debris cloud momentum. Like the 1968 study described previously, they also used a compound ballistic pendulum setup in which the bumper or target plate was mounted to a support frame from which two pendulum plates were suspended. The first plate, located just forward of the target, contained an aperture through which the projectile could travel. This pendulum served as the ejecta catcher and recorded its momentum. Behind the target plate resided another pendulum which served as the recipient to the debris cloud. This pendulum was intended to measure the debris cloud axial momentum. The researchers in this study, as in the previous one, were primarily interested only in the integrated momentum value in the axial direction. This data was then used to verify models developed to predict hypervelocity impact phenomenon at velocities not yet attainable through current experimental methods. This technique is referred to as velocity scaling.

III.2. Momentum Profiles

Although the previously cited studies were primarily interested in the net integrated momentum present in the debris cloud, there have been interests and investigations into obtaining momentum profiles. Recent studies have pointed out the potential importance of

knowing the momentum distribution in the debris cloud in order to determine which portion of the cloud is most energetic and, thus, most likely to cause hull failure[47]. These studies called for a determination of momentum distribution through the use of ballistic pendula arranged in a flat strip configuration. The studies also suggested varying shield materials and configurations to determine their effects upon momentum distribution. From this information, the investigators proposed that models for predicting the performance of bumper shields could be developed. It was therefore determined that the development of a method for obtaining momentum distributions was of critical importance to any successful development of bumper shield designs.

There has been, in fact, studies into this exact subject conducted in the late 1960s by researchers at the Air Force Materials Laboratory[48]. In the research conducted by Swift and Prater, an effort was made to measure both total axial momentum and individual momentum contributions of various parts of the debris cloud. As with the S_wRI study, this was done in hopes of developing ballistic limit equations for velocities which were not yet attainable. The manner in which the individual momentum contributions were obtained involved placing small aluminum blocks or flyer plates in the path of the expanding debris cloud (Figure 3). The blocks were placed on a sheet of film which was in turn exposed by an x-ray source located directly above. The x-ray source was timed to coincide with the impact and propagation of the debris cloud as it propelled the blocks along paths radial to the impact point. Two different exposures were made at predetermined times to permit the calculation of flyer plate velocities. With this information used in conjunction with the plate masses it was then possible to calculate the momentum for each of the discrete region which impacted

the corresponding block. Some success was obtained using this method with results indicating that the momentum profile was triangular in shape, tapering off as the distance from the normal incident increased for the flyer plate method, while the profile was more Guassian in nature for the ballistic pendulum.

III.3. Momentum Multiplication

One of the benefits contrived though the work previously mentioned has been the possibility of verification and determination of a momentum multiplication factor. Although this value does not necessarily correlate directly with the ability of a bumper to "spread" momentum of an impacting particle, it does permit researchers an opportunity to further understand the process by which momentum is transferred. Basically, momentum multiplication is the phenomenon associated with hypervelocity impacts in which the momentum of the debris cloud is larger than the momentum of the incident particle. This can possibly be explained by a net mass gain as part of the bumper disintegrates and joins the projectile to form the debris cloud. This is, however, only a possible source for this multiplication factor and therefore serves as an area of interest to researchers. The overall momentum of the system must still be conserved with the increase in forward momentum being compensated by the creation of backscattered ejecta. In a study conducted by Abbot and Bjorkman, an attempt was made to determine this multiplication factor for the impact of an aluminum sphere with an aluminum bumper[49]. This was performed using a two dimensional hydrocode simulation software package known as CSQIII. From their efforts, they were able to conclude that the optimum hull configuration would be one which produced

no rebound upon impact by the debris cloud. This rebound phenomenon is thought to effectively increase the momentum transferred to the hull, thereby increasing the risk of hull failure or penetration. The S_wRI study also determined a momentum multiplication value for their study, but they were in some disagreement with the findings of the Abbot and Bjorkman research. This was probably attributed to the differences between experimental setups and test conditions. It is these discrepancies which at least provided partial motivation for the efforts of this research to determine the potential effectiveness of the FSMMD for calculating such non-extrinsic properties of the debris cloud. Nonetheless, it should be emphasized that it is not the intention of this study to prove or develop theories regarding momentum multiplication but simply to design and develop a device by which this information might possibly be obtained.

The approach used in this thesis represents a combination of all the best features present in these methods while providing an easier platform for making rapid measurements. The information provided in these studies further emphasize the importance placed on determining momentum in the debris clouds and its distribution profile. It is evident that this information is crucial towards developing effective and accurate bumper design criteria.

III.4. Light Gas Gun Systems

In order to accomplish the majority of experimentation regarding the study of hypervelocity impact phenomenon there must exist some means of simulating and recording the impact process. As with this research, the most utilized means of simulation involves the use of the light gas gun. The light gas gun currently serves as the only reliable means by

which a predetermined mass can be launched in the hypervelocity regime while maintaining a nondeforming shape. While other means exist by which higher velocities may be obtained (i.e. plasma discharge launchers, rail guns, etc.), only the light gas gun is capable of providing the researcher with a relatively simple yet effective means for impacting projectiles with targets at speeds up to 8 km/sec. Unfortunately the light gas gun system is not well suited for obtaining velocities much above this. However, it is a relatively simple tool for investigating impacts in the hypervelocity region.

The light gas gun is similar to the ordinary powder type guns in that it relies upon the rapid expansion of gases to propel the projectile along a flight tube or barrel. Unlike powder guns, however, the light gas gun takes advantage of the extremely high flow rates achievable with low molecular weight gases such as helium and hydrogen to produce hypervelocity projectiles[50]. The basic operation behind this configuration consists of a primary stage containing the breech and high pressure section. In this stage, the powder charge, squib, and piston are located. The second stage consists of the pump and flight tubes. It is in this stage that the high pressure light gas (H_2 or He), the burst or rupture disk, the sabot, and the projectile are located.

The operation of the two stage light gas gun consists of placing the projectile, which is typically a sphere or disk in shape, into a sabot or a supporting jacket. This is done to insure that an adequate seal within the flight tube is maintained and to prevent any interaction of the rapidly expanding second stage gas with the projectile. In some cases, the sabot is comprised of multiple pieces and is allowed to fall free after exiting the barrel. In the case of this study, the sabot is mechanically "stripped" from the projectile by tungsten blades.

This allows the projectile to continue along the flight path without the possibility of it being accompanied by sabot fragments. The projectile-sabot assembly is placed at the entrance to the flight tube just aft of the burst disk. The burst disk is a small metal plate scoriated in the center which separates the compressing light gas in the pump tube from the sabot located in the flight tube until a critical pressure is obtained. The next stage of operation involves the loading of a piston into the high pressure section. It is placed at the beginning of the pump tube and followed by the powder charge. Once the squib or igniting wire has been placed in the charge, the breech cap is put in place and the light gas is introduced into the pump tube. This is continued until a certain specified pressure is obtained. In addition to these steps, the target test chamber is evacuated and all photographic and timing devices are reset.

The operation of the two stage light gas gun begins with the application of current to the squib which in turn ignites the powder charge. The rapidly expanding gases generated by this explosion act to force the piston into the pump tube section. This results in a quick compression of the light gas in the high pressure section just ahead of the piston. The primary pressure source continues to build until a critical pressure predetermined by the burst disk is obtained. Upon the rupturing of the burst disk, the highly pressurized light gas is released to flow into the flight tube forcing the sabot-projectile combination down range. At a specified point, the sabot is removed and the projectile is allowed to continue into the range tank area where the target(s) are located. The timing and photographic equipment are typically triggered electronically.

III.4.1. LGG Photographic and Timing Methods

There are several methods available for photographing the projectile as it leaves the barrel and passes into the test chamber. The two most popular methods include the flash camera and the smear camera[51]. Each of these are capable of producing a photographic image representative of the projectile permitting the accurate determination of velocity. The flash camera is comprised of an ultra-high speed illumination source and a piece of film which resides on opposite sides of the projectile. The source is triggered electronically to coincide with the passage of the projectile, exposing the film except where blocked by the projectile. Using an x-ray generator such as the vacuum-arc flash x-ray tube, exposure times as short as 2×10^{-7} seconds are attainable. The use of x-ray as an illuminating source allows for the exclusion of such firing by-products as smoke and non-metallic sabot material. There is, of course, the limitation that only metallic objects can be observed with this method. Since the primary materials investigated in hypervelocity impact studies are metallic, this has not prohibited its utilization as both a timing and projectile observation technique. The streak or smear camera is another of the more predominantly used methods for obtaining projectile velocities. Unlike the single image exposure produced by the flash camera technique, the image of the projectile is "smeared" along a continuously exposed piece of film. A plate separates the projectile from the film and allows light to pass only through a slit located in the center. In this fashion, the film is only exposed as the line source of illumination crosses it transversely. The film is moved at a constant velocity producing a streaked image of the projectile as it breaks the beam of illuminating energy. The output of this method is essentially a position vs. time plot of the projectile through a certain specified

distance and can be used to calculate velocity. It cannot, however, distinguish characteristics of the projectile such as deformation or fragmentation.

These methods are used primarily to characterize the motion of the projectile as a means of velocity determination. Although the flash camera is capable of capturing the debris cloud as it is produced, other methods exist which are better suited for this purpose. The fastest of the high-speed photographic techniques is the rotating mirror camera. Utilizing this technique it is possible to achieve frame rates as high as one million frames per second with exposure times as small as 5×10^{-8} seconds. This is an ideal method for capturing the debris clouds expansion and propagation over sufficiently small time increments. The concept behind the rotating mirror camera relies primarily upon a centrally located mirror surrounded by a film strip and individual lenses. Each of the relay lenses acts as an individual camera, capturing one image on the portion of film located immediately behind it. The mirror in the center is attached to a gas turbine which is accelerated to an extremely high velocity. This method typically produces 20-30 images, each separated by only tens of nanoseconds. This technique has produced spectacular photographs of the debris cloud and has allowed researchers to track individual components for velocity distribution data. The limitation to this technique as with the previously mentioned ones is that the image produced on the film is of all of the particles throughout the depth of the debris cloud. This does not permit the separation of velocities for the internal components from the outside ones. Lately, researchers have demonstrated techniques for "slicing" the debris cloud into a thin layer using plates to block the remainder of the cloud[52]. Thus enabling the accurate determination of velocity distributions. This technique, used in conjunction with the actual physical

monitoring of momentum (through the use of the FSMMD) would provide a thorough and accurate analysis and characterization of the debris cloud.

IV. EXPERIMENTAL SETUP

The experimental setup for this study consisted primarily of two distinct areas, the hypervelocity impact facility and the focus of this study, the forward scatter momentum monitoring device. The hypervelocity impact facility which is under the operation of the NASA Marshall Space Flight Center, provided the use of a two stage light gas launcher for this study along with various support personnel and instrumentation which were instrumental in its success.

IV.1. Space Debris Simulation Facility (Light Gas Gun)

The Space Debris Simulation Facility (SDSF) located within the Materials and Processes Laboratory at the NASA/Marshall Space Flight Center is a facility built with the specific intention of performing hypervelocity impact studies for spacecraft protection research [53]. Originally designed as a micrometeroid simulation facility, it was converted to test man made debris impacts in 1985. It consists of a two stage light gas gun, test chambers, flash x-ray, Hall station, and rotating mirror cameras, and all instrumentation related to its operation. The gun is capable of propelling projectiles with masses ranging from 4 to 300mg at velocities between 2 and 8.0 km/sec. The projectile diameters may range from 2.5 to 12.7 mm with barrel diameters of 6.35 and 12.7 mm available.

IV.1.1. SDSF LGG Specifications

The specifications for the SDSF light gas gun are as follows. The breech section (8.89 cm inside diameter by 60.96 cm length) which is capable of withstanding 50,000 psi internal pressure (typically kept beneath 20,000 psi during standard testing) serves to contain the primary (powder charge) or first stage pressure generator. This is followed immediately by the pump tube section (6.35 cm i.d. by 3.048m length) which contains a nominal pressure of 100 psi H_2 light gas in front of a polyethylene piston. This section serves as the secondary or second stage pressure source.

Following this second stage is the high pressure section which tapers from the pump tubes' diameter to the diameter of the barrel. This is followed by a metal burst disc. The barrel (6.35 or 12.7mm dia. x 2.59m long) immediately proceeds the burst disc. The barrel culminates into a $0.067m^3$ test chamber followed by an additional $0.53m^3$ intermediate test chamber. For extremely large objects, a $28.5m^3$ pressure tank is located just behind the second test chamber.

IV.2. SDSF Light Gas Gun Operation

The operation of the SDSF light gas gun begins with the ignition of approximately 200-300 gm of M1, Class B, 1.3C slow burning high explosives. This results in a pressure increase within the breech to a predetermined level at which point the piston is released. The piston is accelerated to a velocity of approximately 900 m/sec compressing the H_2 gas located in the pump tube[54]. This process occurs until the burst disk ruptures at a predetermined pressure and allows the gas to flow into the barrel. This in turn produces the

force required to move the projectile. To compensate for the decrease in pressure which occurs with the gas flow into the barrel, the high pressure section is tapered and effectively increases the pressure as the piston moves further down the pump tube. The critical variables in maintaining accurate operation of the SDSF light gas gun are propellant mass, piston mass, light gas (H_2) pressure, projectile mass, and burst disc pressure limit. These must be kept within tight restrictions in order to reproduce accurate and predictable velocities.

IV.3. Velocity and Debris Cloud Monitoring Equipment

The SDSF is equipped with several methods for velocity determination including an x-ray flash camera unit, a piston velocity detection system, and a Hall Station high speed camera operating in streak mode. The x-ray flash system is used for projectile velocity determination by producing three consecutive images of the projectile. These are recorded on three pieces of film by exposed individually by an x-ray source. This source exposes an area (25.4 mm x 457 mm) containing the projectile image and a timing mark common to all three exposures. This mark is used as a common reference point for each image. These images are then used in conjunction with data produced by three time interval counters to determine projectile velocity. The Hall Station camera is also used to determine projectile velocities by exposing a moving piece of film to a line source blocked by the projectile during its flight down range. This results in a streak image of the projectiles position as a function of time.

The SDSF is also equipped with a Cordin 330IR high speed rotating mirror camera. This

camera is capable of exposures rates in the vicinity of 1 million frames/sec. Utilizing this system, it should be possible to accurately photograph and observe the production and propagation of the debris cloud in great detail. Unfortunately, the Cordin system is highly complex and is requires several modifications to the SDSF light gas gun test chambers to facilitate it's accurate implementation. However, when this system becomes available for use, it will provide a vital service in providing complimentary data to that produced by the FSMMD to characterize the debris cloud.

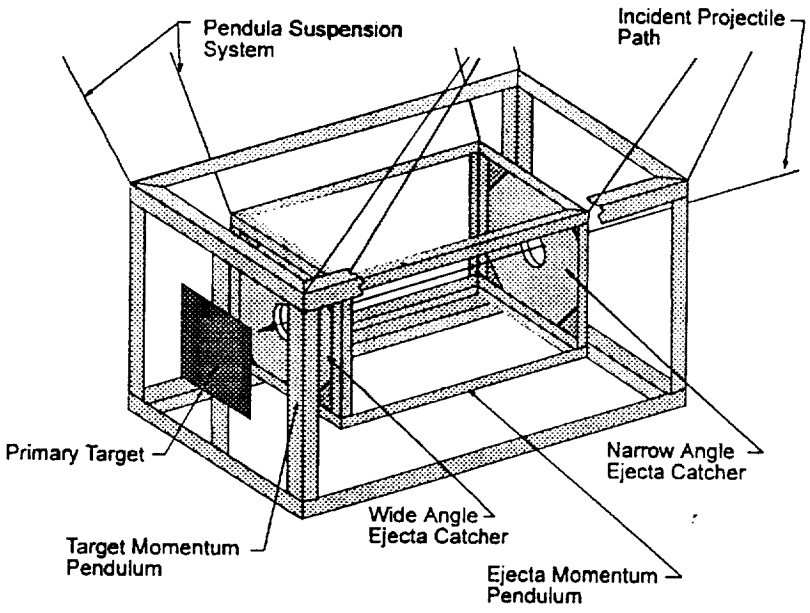

Figure 2. Compound Ballistic Pendula for Measuring Bumper/Ejecta Momenta

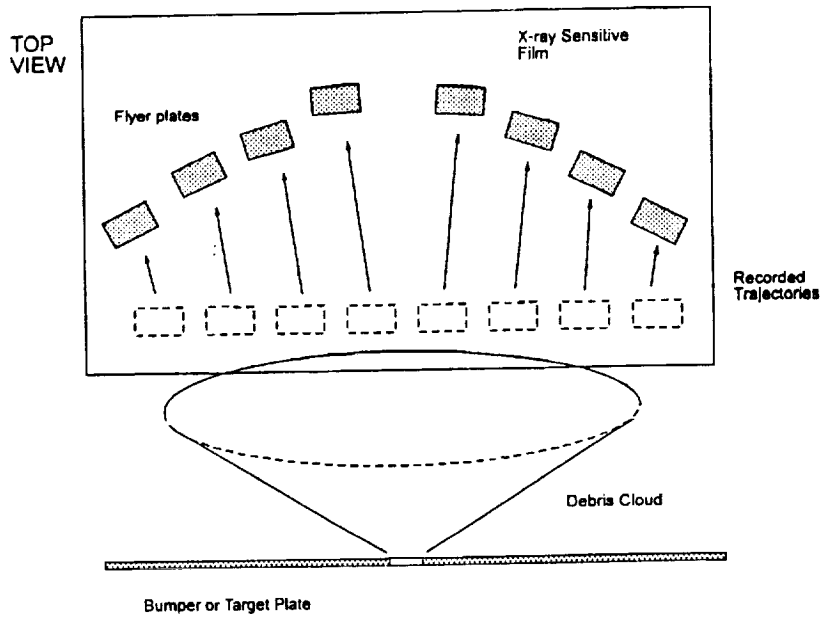

Figure 3. Flyer Plate Type Momentum Density Measuring System

V. RESULTS AND DISCUSSION

The results presented in this section represent the cumulative effort involved in the design and development of the Forward Scatter Momentum Monitoring Device (FSMMD). It must be emphasized that the detailed analysis of debris cloud momentum distributions and their corresponding dependence upon experimental parameters is beyond the scope of this study. The experimental results given here are for verification and validation of the ideas and concepts utilized. Further research and future recommendations for debris cloud investigations are given in the appropriate segment of this thesis.

V.1. FSMMD Design and Development

The design and development of the FSMMD can be traced through four distinct design phases with each phase producing a prototype design and corresponding instrument. The fourth and final phase resulted in the current FSMMD design which is now in use at NASA's Marshall Space Flight Center in Huntsville, AL. The following exert will trace the design and development process as it progressed from the prototype stages (PMD-1 through PMD-3) to the final design (FSMMD).

V.1.1. Initial Design (PMD-1)

At the onset of the effort to characterize the debris cloud, it was originally intended to measure both energy and momentum.[55] This resulted in the design of a device to test certain fundamental system concepts on how best to accomplish this task. The first prototype momentum device, designated PMD-1, consisted of both energy and momentum sensors.

Each was accompanied by a duplicate sensor to provide for a total of four. The steel plate located just prior to the sensors served to shield the components from the debris cloud and gas surge while allowing only a discrete portion of the cloud to reach each of the sensors.

The energy sensors consisted of a hollow aluminum cylinder with four strain gauges placed at 90° intervals around the circumference. The end of the cylinder was covered by a 3/8" diameter stainless steel cap which served to collect the portion of the incident debris cloud of interest. Each cylinder was then threaded into a steel support block which in turn was mounted to the base plate. The concept to be employed would encompass taking measurements of strain after impact by the debris cloud to determine the amount of energy deposited by the debris upon the sensor. The use of four strain gauges in the previously mentioned configuration was intended to indicate if bending of the rod occurred in the event that non-uniform compression of the sensor takes place. The data from the gauges were to be taken by strain indicators and then zeroed for the next test by re-balancing the bridging circuit. The momentum sensors tested on the PMD-1 consisted of a series of ballistic pendula suspended from a steel axle and protected from the debris cloud by a blast shield. Each pendulum consisted of an aluminum pendulum arm, impact block, and timing blade. The principal for operation of the momentum sensors relied upon the transfer of momentum from the incident debris onto each pendula impact block. As with the energy sensors, the debris cloud was blocked at all points except for a 3/8" diameter region located centrally on the impact block. The momentum imparted upon the impact block produced a resulting motion in the pendulum which was then recorded using a timing and data collection system. The timing portion of the pendulum consisted of an aluminum blade with slots placed at

regular intervals along its lower edge. These gaps serve to block and expose the infrared beam produced by one side of a photo-interrupter diode which is then detected by the sensor on the opposite side. The diode was positioned just behind the timing blade and in the path of the arc traced by the blade and possessed a 1/8" gap located between the emitter and the detector thus providing a path for the timing blade to pass through. The signal output of the diode in the exposed position was 5V DC while the output was 0V DC during the blocked position. Thus, the intermittent blocking and exposure of the infrared beam produced by the emitter and received by the detector , produced a square wave signal when observed during a trace on an oscilloscope. By utilizing the information regarding the time scale produced by the oscilloscope readout and gap sizes from the timing blade, the instantaneous velocities as each gap passes through the diode is determined. Using simple physical relations regarding angular and linear momentum, the momentum of the incident debris is then obtainable.

As stated earlier, the first prototype was designed primarily as a platform by which these sensors could be developed and tested. Preliminary results from the first series of tests indicated that the energy sensors were not sufficiently robust to be of any significant value. This, compounded with the innate difficulty which existed in fabricating the sensors prompted the decision to concentrate solely upon momentum measurements. Thus, all devices built after this point contained momentum sensors exclusively. While the energy sensors proved to lack required durability, they did provide some data which would indicate that further development could provide a useful sensor for characterizing the energy throughout the debris cloud. Unlike the energy sensors, the momentum sensors proved to be considerably more reliable and showed great promise for further design improvements. The

primary difficulties exhibited during the initial testing consisted of the lack of rigidity in the pendulum assembly and the difficulty in triggering the oscilloscopes at the correct moment. Thus, these as well as several other problems served as the sources for further design improvement for the following design phase.

V.1.2. PMD-2

After the testing of the preliminary designs for the momentum and energy sensors implemented on PMD-1 was completed and analyzed a new device was designed and constructed. The new design consisted of an expanded version of the momentum sensors with the number of sensors being doubled to four. As mentioned earlier the new design concentrated entirely upon momentum measurements and eliminated any attempts to measure energy. This allowed for the examination of a larger area of the debris cloud as well as the acquisition of a more dense data scatter than was possible with the PMD-1. The PMD-2 consisted of four pendula located at angles of 10°and 20° to one side of the normal incident direction and 15°and 25° to the opposing side. This permitted a more thorough examination of the debris cloud while maintaining a minimum of sensors. Figure 4 illustrates the design and layout of the PMD-2 device. Some of design improvements implemented in the PMD-2 that were not present in the PMD-1 include the use of shielded precision bearings to reduce the affects of friction upon pendulum performance.

Another design innovation used in the PMD-2 involved the division of the blast shield into three separate pieces. This provided the capability to replace only those portions of the

blast shield which were severely damaged while allowing the undamaged pieces to be further utilized. This also simplified the manufacture of the blast shield and made it more interchangeable with other replacement parts. Perhaps the most significant improvement over the PMD-1 design was the total redesign of the pendulum assemblies. In the previous model, the pendula were designed to be held together by press-fitting the pieces to one another. This was required in order to allow for on-the-spot adjustment when necessary. During the testing of the PMD-1, the press-fit pendulum assemblies were unable to withstand the shock being imparted on them without coming apart. It was therefore decided that a rigid assembly was required and thus a closer tolerance on the pendulum systems was in order. The redesign yielded a pendulum assembly comprised of essentially the same components as in the PMD-1 (pendulum arm, impact block, and timing blade) but were fastened together with screws. This permitted little if any adjustment and thus required that the placement of the photo-interrupter diodes be much more precise than before. In addition to the enhancement in rigidity of the pendula, the components themselves were enlarged slightly to provide for longer life and greater durability. The design for securing the bearings within the pendulum arm was modified to include a set of three set-screws located 90° apart. Each bearing was retained in its proper position along the axle by two securing nuts with set-screws. The entire PMD-2 was enclosed within an aluminum cover to help shield the effects of the gas surge and flash produced by the burning sabot material. The photo-interrupter diodes were connected to the exterior of the test chamber via a flanged vacuum fitting/pinned connector combination. The leads were attached to the connector with gold plated pins on both the outside of the chamber as well as the inside. All power to the

device as well as signal output channels passed through this connector. As with the PMD-1 momentum sensors, the PMD-2 data output was observed and recorded with two digital storage oscilloscopes. Triggering was accomplished by manually setting the trigger voltage just prior to the test event. This proved to be difficult to perform and unreliable. During the final stages of preparation for firing the LGG system, the pump tube is filled with hydrogen which is then maintained at a fairly high pressure. Due to NASA safety requirements, all personnel are prohibited from entering within close proximity of the pump tube and the test chamber which precedes it. Thus all adjustments to the oscilloscopes were required prior to the application of the high pressure to the pump tube. In addition to this difficulty, it was observed that the closing of the range tank valve located above the test chamber isolating the target chamber from the vacuum pump was prematurely triggering the oscilloscopes. This problem was addressed by running coaxial cables to the test chamber and operating the oscilloscopes from within the control room. This, however, did not eliminate the difficulty in triggering at the correct moment to ensure capture of the entire data sweep. These problems were addressed in the design and development of the third prototype device (PMD-3). Although data acquisition was hampered by the aforementioned difficulties, the mechanical design of the PMD-2 proved to be more than satisfactory. There were little or no adjustments required for the mechanical assemblies until after three tests had been conducted. The blast shields were replaced after approximately four to five tests. An instance did arise, however, in which a particularly damaging debris cloud managed to spall the edge of an aperture and caused failure of a photo-diode.

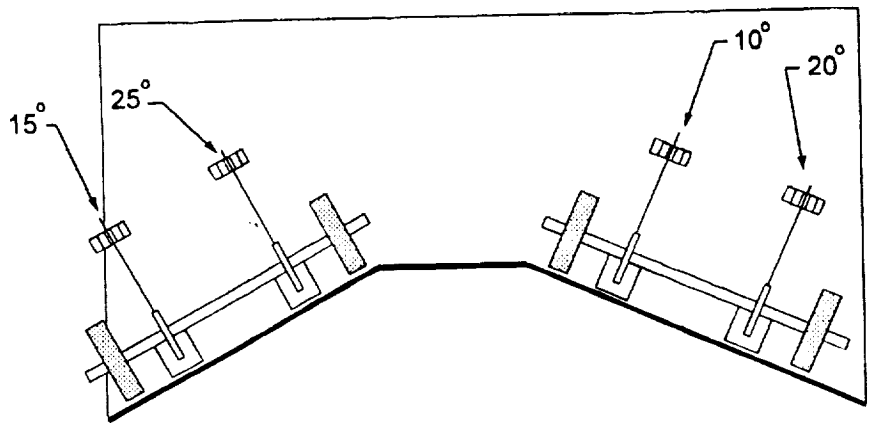

Figure 4. PMD-2 Design

V.1.3. PMD-3

The third redesign of the momentum measuring device was designated as PMD-3 and consisted of six pendula. This device was essentially the same as the previous prototype (PMD-2), with the exception of the addition of two more pendula. This was decided upon after analyzing the results from the PMD-2 tests. The data from the PMD-2 indicated that there were regions within the debris cloud which could not be accurately characterized with only four data points. This resulted in the inability to determine whether or not the debris cloud was in fact very compact and lacking radial expansion or consisting of large chunks of solid matter. Both of these conditions would give rise to rather high momentum readings near the center of the momentum distribution curve with the data points dropping off

considerably as the radial distance from the center of the debris cloud increased. Therefore, it was decided to add two additional pendula to increase the data density. Figure 5 shows the PMD-3 layout in conjunction with the placement of the device with respect to the bumper and incident projectile. The pendula were added to measure the debris momentum at 30° and 35° from the normal incident direction of the projectile prior to impacting the bumper. It was this configuration which was utilized to examine a series of test conditions which would in turn provide calibrating information as well as an initial examination into the device's sensitivity to such parameters as projectile diameter, impact velocity, and bumper thickness. With the PMD-3, more than sixty shots were completed with a test series of sixteen shots which provided data for actual bumper analyses[56]. One of the primary concerns in the development of the PMD-3, was to improve upon the instruments durability and turn-around time between overhauls. This was deemed necessary in that in order to be a useful laboratory instrument it must be easy to assemble and set-up as well as possess the ability to make several tests in rapid succession with a minimum of adjustment. This requirement arose due to the difficulty in operating the LGG system in a timely fashion. A total of four to five shots could be attempted in a day with three to four being more reasonable. This was dependent of course upon the quickness of installing and resetting of any instrument located in the test chamber. The connection and disconnection of the PMD-3 took approximately thirty to forty five minutes and thus it's removal after each shot for repair or adjustment would reduce the number of shots possible in a day to barely two. Thus the reliability requirement became an essential goal in producing a useful instrument for space station bumper analyses.

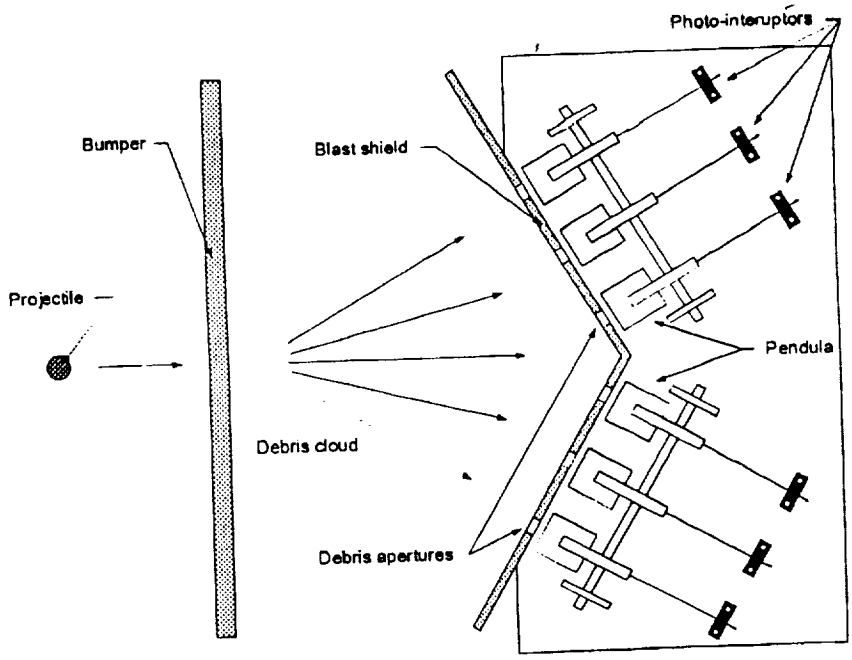

Figure 5. PMD-3 Design and Experimental Setup

V.1.4. FSMMD (PMD-4)

The fourth and final device constructed for this study was designated the FSMMD (Forward Scattering Momentum Measuring Device). It is an improvement upon the PMD-3 which proved to be a sound design and capable of making useful measurements in characterizing the debris cloud momentum distribution. The FSMMD consists of eight

pendula located along a six inch radius at positions enabling measurements to be made at 5° intervals beginning at 5° from the normal incident direction of the incoming projectile and ending at 40°. This increased the data yield provided by the PMD-3 by two more measurements. Unlike the PMD-3, the FSMMD is configured along a radius insuring that all pendula will witness their respective normally incident debris. This design improvement was made in order to fine tune the measurement accuracy provided by the PMD-3. The FSMMD now represents the final stage in the design and development of a momentum measuring instrument for use in debris shielding analyses. Current work is under progress to develop a BSMMD (Back Scattering Momentum Measuring Device) in order to examine the total momentum distribution in the debris cloud. With the completion of this instrument, a method for characterizing the debris cloud will finally be possible enabling a more detailed analysis of the impact phenomenon and providing an experimental verification of the numerical simulations currently being employed.

V.1.5. Device Testing and Usage

As mentioned previously the PMD-3 was utilized over sixty times yielding useful data for more than twenty five of those tests. The other tests were disregarded due to error introduced by anomalies in the LGG system or incorrect connection of the data collection system. The test series examined with the use of the PMD-3 consisted of a matrix in which the following variables were used: projectile velocity, bumper thickness, and projectile diameter. Each of the tests conducted for a particular set of conditions was repeated at least once to verify their accuracy. The experimental set-up for these tests consisted of aluminum

spheres (1100 Al) fired by the LGG system at bumper plates (6061-T6 Al). This represented the current space station configuration being examined by NASA. The PMD-3 was placed in the secondary test chamber located just prior to the main test chamber. The bumper plate was placed at a distance of 15.24 cm (6") from the front of the blast shield protecting the device. During the tests, the chamber was evacuated to a vacuum of 300 millitorr or less. The primary impact between the aluminum projectile and bumper produced a high energy debris cloud, the distribution of which is the center of investigation in this section.

V.2. Backward Scattering Momentum Monitoring Devices

The backward scattered momentum monitoring device(BSMMD) was altered for each of the three series of experiments. The shape of the backward scattered debris cloud, i.e. conical, allowed for a single plate with a hole to be used. If the collector plate has a large enough standoff distance from the bumper plate than no backward scattered debris will go back through a passage hole. This distance was determined through review of hypervelocity impact debris cloud photographs to be approximately two inches.[24]

All three designs consisted of 6061-T6 aluminum plates with two inch diameter passage holes. The two inch passage holes were necessary due to the inability of the LGG to precisely control the path of the projectile. Coupled photo interruptors were also used for all three devices as the means of measuring the angular velocity of the collector plate pendulum. The basic design of the backward scattered devices can be seen in Figure 6.

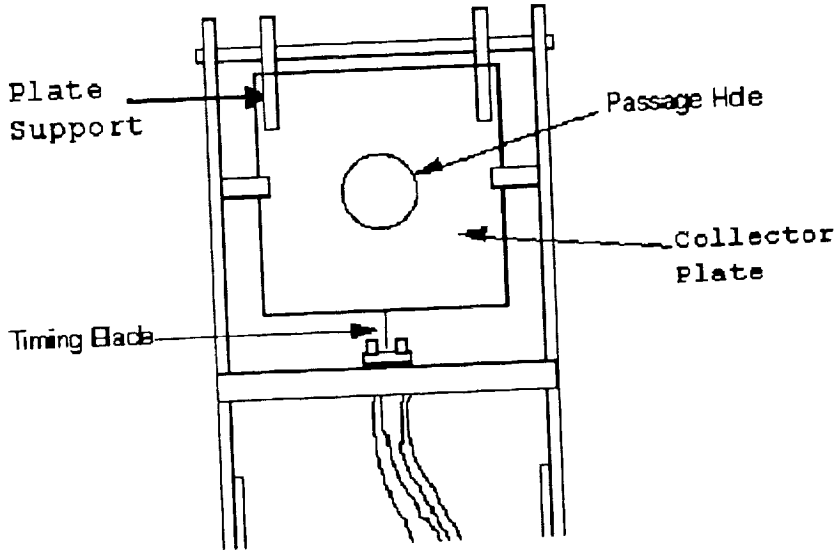

Figure 6. Backward Scattered Momentum Device

The original device had two plate supports. The original device's plate supports were positioned closer together with respect to the plate than the device shown in Figure 6. The initial plate support also only extended down far enough onto the collector plate to allow one bolt for attachment. The dimensions of the collector plate for the initial set of experiments, Z101-Z108, was 6" by 6" by 1/8" thickness.

For the second set of experiments, Z201-Z208, it was decided that individual backward scattered plates would be machined for each experiment. This would provide evidence of substantial mass gain if it were to occur. It would also give a permanent physical record of

the shape of the back scattered debris cloud. The plate dimensions were increased to 6.5" X 6.5" X 1/8" to ensure that all of the backward scattered debris was being collected.

An additional plate support located at the horizontal center was also added for the 200 series of tests. It was felt that decreasing the length of the moment arm would reduce the effects of off-centered shots. The plate supports were also extended down further onto the plate and used an additional bolt in each to hold the backward scattered collector plate.

These design modifications were made in hopes of improving the rigidity of the system. Improving the stiffness of the BSMMD helped restrict the angular motion of the back scattered pendulum to a particular arc along which the coupled photo interruptors were placed. The final design can be seen in the following photograph (Figure 7). For the last set of experiments it was decided that the middle plate support was unnecessary but that the additional bolt in the legs of the plate support had provided needed stiffness. Also for this series individual back scattered collector plates were machined for each experiment. The plate dimensions, the same as for the 200 series of experiments were 6.5" x 6.5" x 1/8" made from 6061-T6 aluminum.

The first two backward scattering momentum monitoring devices required a vice to stabilize their position in the chamber. Another change made for the final BSMMD is that it had its own base. This allowed the backward scattered collector plate to be moved closer to the bumper if desired.

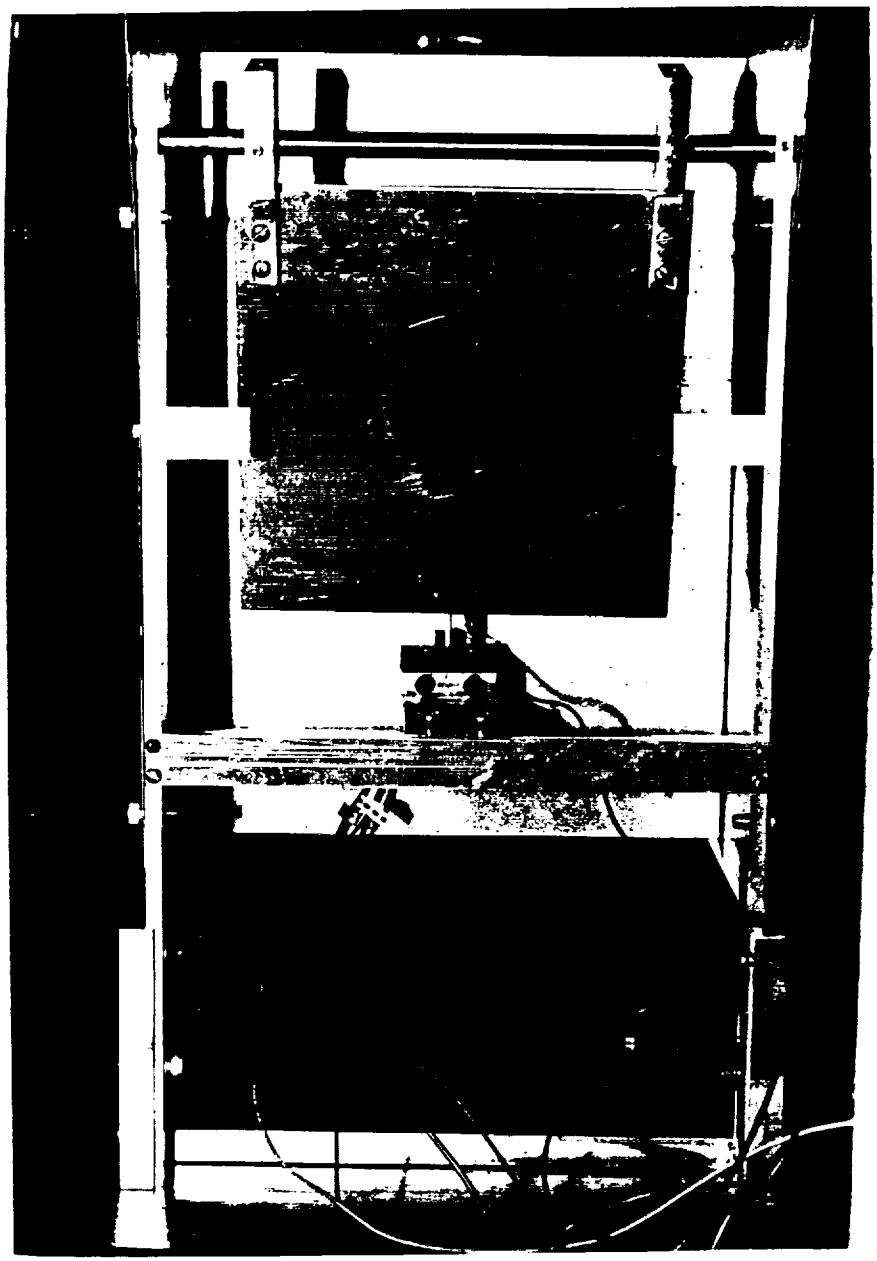

Figure 7. Backward Momentum Monitoring Device

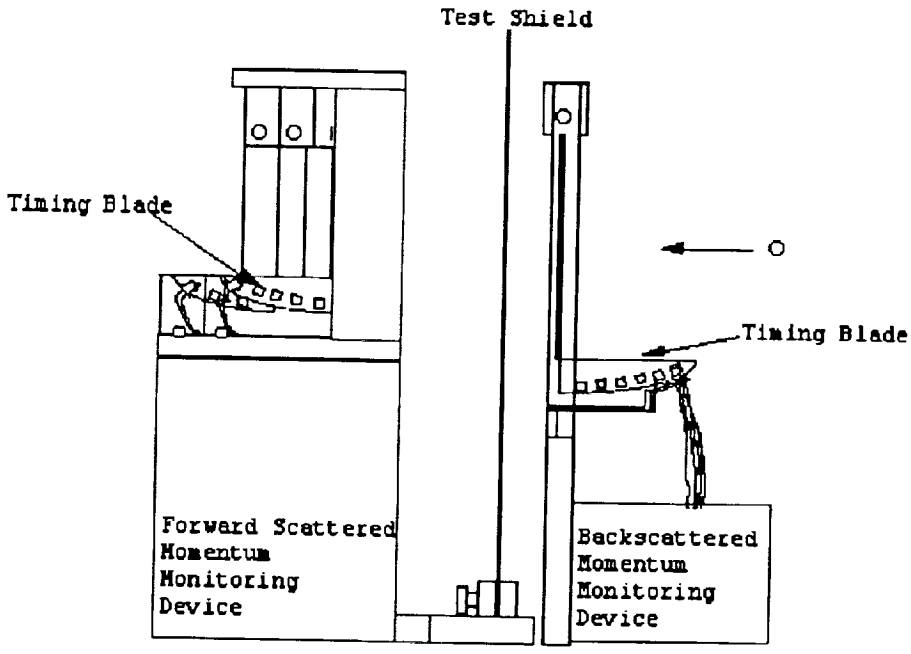

Figure 8. Side View of Chamber Setup

V.3. Momentum Determination and Data Collection

Although over sixty shots were made during the development of the FSMMD, the following results include only those tests involving 0.635cm (0.25in) diameter projectiles with velocities between 5 and 7.2 km/sec. These conditions were determined to be most appropriate towards evaluating the FSMMD operation in that the debris cloud generated by these conditions tends to be relatively uniform and free from large fragments. The following table shows the conditions for all of the successful shot attempted and their corresponding data. The gaps in the numbering system represent those shots in which a gun malfunction or other major technical problem occurred thus preventing the acquisition of data. The thickness of the bumper panels ranged between 0.1016cm (0.040") and 0.2032cm (0.080"). Data collection and storage was accomplished through the use of a digital storage oscilloscope. During the testing phases of both the PMD-1 and the PMD-2, two oscilloscopes were utilized to record four channels of data, one channel for each pendulum. When the design was altered to include six pendula, it soon became evident that this method of recording data would not be feasible. Fortunately, access to a Norland A-200i digital oscilloscope was made available by NASA enabling the recording and storage of up to ten channels simultaneously. Triggering was accomplished by inputting the signal produced by an x-ray flash detector used in determining projectile velocity into an extra channel on the scope. Total time duration for data acquisition was approximately two seconds which provided a great enhancement on the previous system. This time period proved to be more than sufficient to allow for all of the pendula to pass through their upward and downward arcs at least once. This was a beneficial effect presented by upgrading to the Norland.

Table 1. FSMMD Testing and Data Summary

Test #	Proj. Dia.	Proj. Vel.	Bumper Thick.
Z44	.313	.6.0	.040
Z53	.313	6.0	.040
Z46	.313	7.2	.040
Z56	.313	7.2	.040
Z45	.313	7.2	.080
Z55	.313	7.2	.080
Z42	.313	6.0	.080
Z54	.313	6.0	.080
Z48	.250	6.0	.080
Z39	.250	6.0	.080
Z51	.250	6.0	.080
Z50	.250	6.0	.040
Z47	.250	6.0	.040
Z31	.250	7.2	.040
Z38	.250	7.2	.040
Z32	.250	7.2	.080
Z33	.250	7.2	.080
Z26	.250	5.0	.040
Z1.31191	.250	6.5	.080
Z2.31191	.250	7.0	.080
Z3.31191	.375	6.65	.080
Z24	.25	6.0	.050
Z1.41591	.25	5.0	.080

V.3.1. Momentum Conversion

The PMD-3 basically monitored the angular movement of each of its momentum sensors (ballistic pendula) induced by the debris cloud upon impact. This motion is directly related to the momentum transfer from the specific portion of the debris cloud to its respective pendulum. It is therefore necessary to determine the conversion factor from angular velocity to momentum density which is denoted in this case as P'. The angular momentum of the discrete portion of the debris cloud (mv) must equal the angular momentum present in the pendula after impact as stated below in equation [2]. It is important to note the distinction between the debris momentum (mv) and the incident projectile momentum ($m_o v_o$).

$$(mv) = \frac{I\omega}{r} \qquad [2]$$

where

$$\omega = \frac{v}{R} \qquad [3]$$

Substituting equation [3] into [2] yields the following equation correlating the momentum of the incident debris (P) with its velocity (v).

$$P = \frac{Iv}{rR} \qquad [4]$$

where: P = mv (debris momentum)

R = radius of arc traced by timing blade

v = velocity of timing blade

r = distance from center of impact block to center of pendulum axis

I = moment of inertia for pendulum

The values of these variables on the right side of equation [4] are given in Table 2.

Table 2. Experiment Constants for FSMMD

R	r	I
13.02 cm	8.89 cm	4285.7 gm cm^2

Substitution of these values into equation [4] yields equation [5].

$$P(kg\frac{cm}{\sec}) = A * v \qquad [5]$$

where A=0.380. Therefore, multiplication of the measured velocity (v) by the constant (A) gives the desired momentum values. This constant is a function of the inertia of the pendulum which was experimentally determined. To obtain the normalized value for momentum per unit area (P'), the momentum values (P) determined in equation [5] are divided by the area of the corresponding aperture in the blast shield which is the area of the impact block exposed to debris. It is also necessary to resolve the momentum per unit area(P') into the component acting in the direction of the incident projectile if momentum multiplication calculations are to be performed. This is simply done by taking the cosine of the momentum per unit area thus giving an effective momentum per unit area (P_{eff}).

Using the previously described method and equation [5], it is possible to calculate the momentum values from the velocities obtained for each pendulum. In the test conducted prior to Z47 the size of the blast shield apertures were maintained at 0.9525 cm (0.375 in.) diameter. In the subsequent tests, the aperture sizes were varied from 0.9525 cm (0.375 in.) to 1.27 cm (0.5 in.) diameter. This was done to increase the probability that the pendula located at the most extreme angles (30° and 35°) would encounter some component of the debris cloud. The data was normalized accordingly for those tests and are given in Table 4.

V.3.2 Preliminary Results for Concept Verification.

Table 3 summarizes the conditions for the tests conducted for verification of the FSMMD concept and design. All of the projectiles utilized in this test matrix possessed a diameter of 0.635cm. Two different bumper thicknesses along with two velocities were employed resulting in a total of four separate and distinct test conditions. Figures 9 through 12 represent the momentum distributions obtained using the previously described method for calculating momentum from pendulum velocities as well as their corresponding raw data. It was evident from these momentum profiles that the greatest values resided near the center of the plot corresponding to that portion of the debris cloud traveling along the projectile axis. These profiles can be approximated by either a Gaussian or triangular data fit within the limit of experimental accuracy. However, the expected symmetry in these profiles was not always evident. This is due in large part to the variations present in the LGG system with respect to its ability to repeatedly fire the projectile at the same location on the bumper plate with fine accuracy. The peak values often shift towards one side or the other of the expected center.

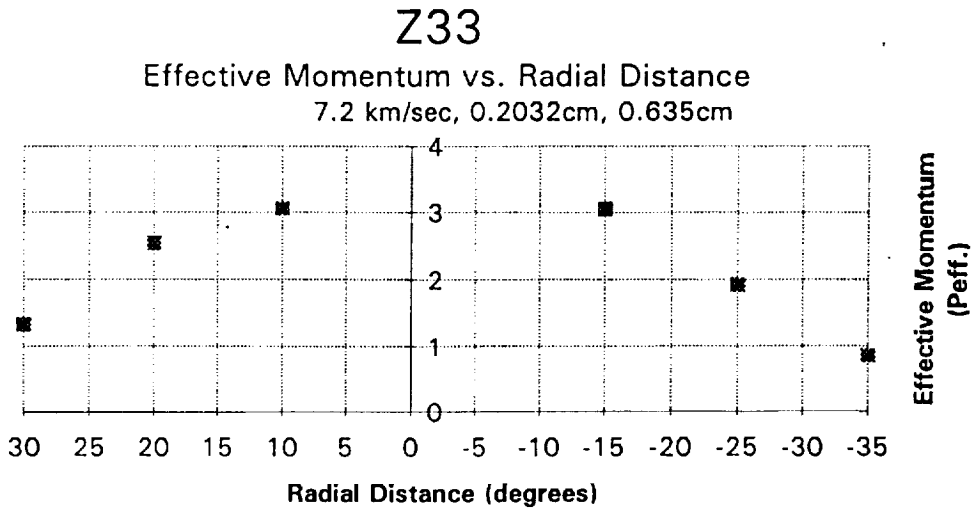

Figure 9. Z-33 Momentum Profile

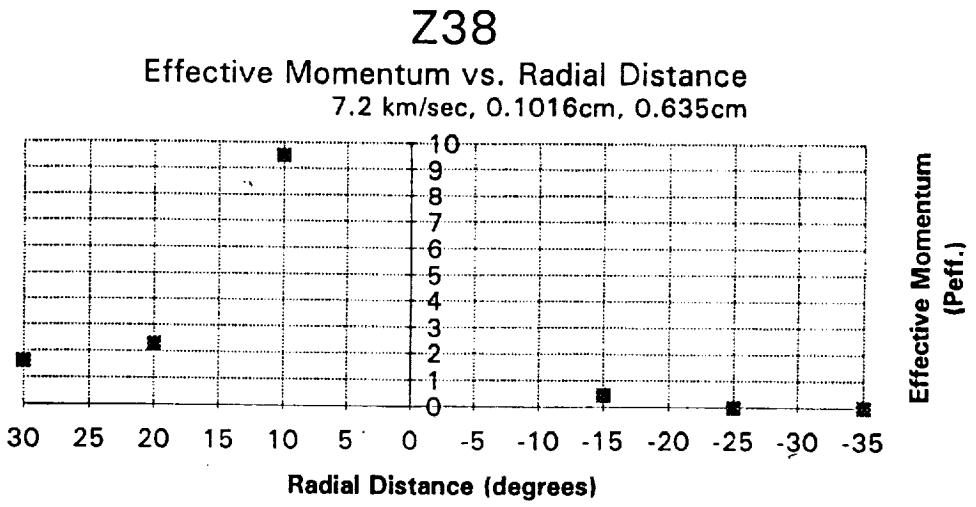

Figure 10. Z-38 Momentum Profile

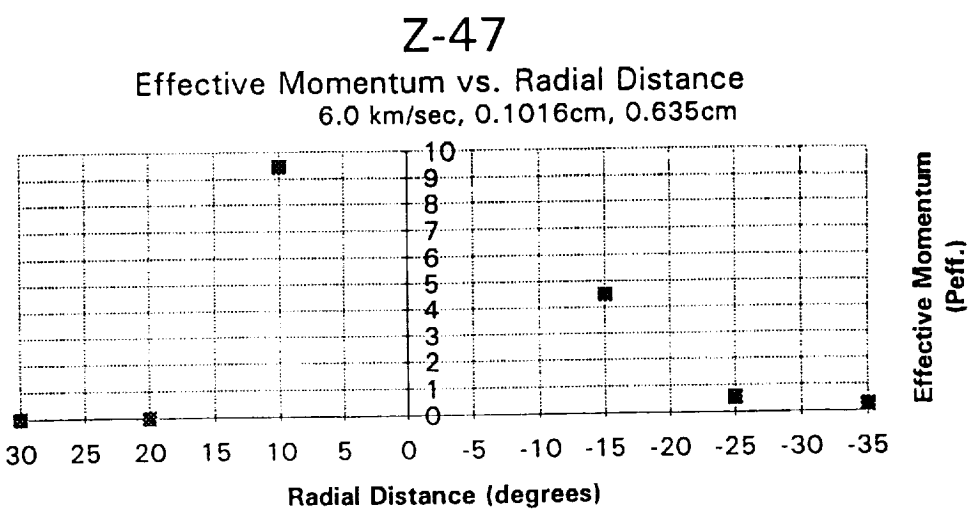

Figure 11. Z-47 Momentum Profile

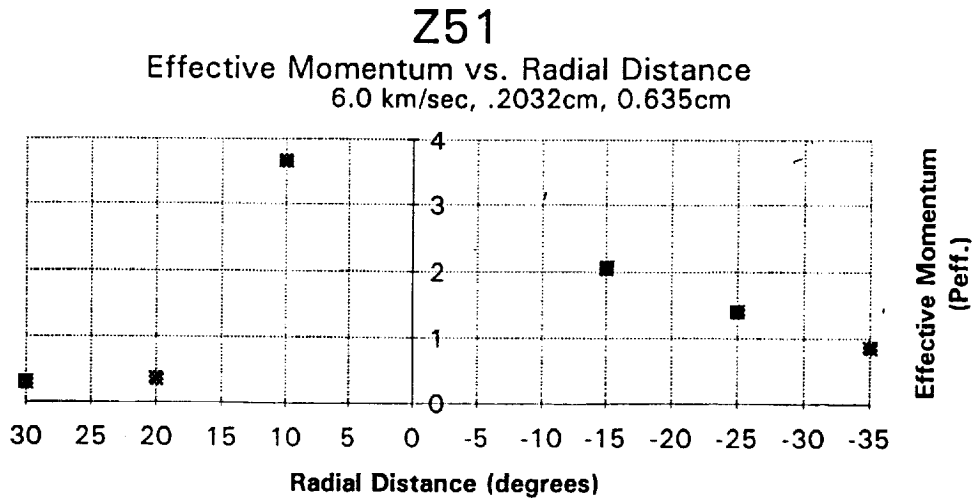

Figure 12. Z-51 Momentum Profile

Table 3. Validation Testing Conditions for FSMMD

Projectile diameter	Bumper thickness	Projectile velocity
0.635cm (0.25in)	0.1016cm (0.040in)	6.0 km/sec
0.635cm (0.25in)	0.2032cm (0.080in)	6.0 km/sec
0.635cm (0.25in)	0.1016cm (0.040in)	7.2 km/sec
0.635cm (0.25in)	0.2032cm (0.080in)	7.2 km/sec

V.3.3. Data Analysis

It appears, that while remaining within the experimental scatter of data, it is appropriate to fit the observed momentum distributions with either a Gaussian or triangular data fit, the latter being preferred due to its inherent simplicity. Such a distribution can therefore be characterized by two parameters: peak value of the momentum per areal density P' and half width (radius r_o) at the base. Total momentum of the debris cloud (P_{tot}) is calculated from these values by integrating the momentum density as described in the following section.

V.3.4. Calculation of Total Momentum

Using the momentum profiles obtained experimentally for the concept verification study, we can calculate the variables P' and r_o described previously. The integration of the momentum density from 0 to r_o is given by equation [6].

$$P_{tot} = \int_o^{ro} 2\pi r(P' - Br)dr \qquad [6]$$

where r = radial distance from normal incident and B = slope of line connecting r_o and P'. This definition of the variable B yields the following equation [7] which then can be substituted into equation [6].

$$B = \frac{P'}{r_o} \qquad [7]$$

Following this substitution and subsequent integration of equation [6] we arrive at equation [8] which represents the total integrated momentum (P_{tot}) for the debris cloud.

$$P_{tot} = \frac{\pi P' r_o^2}{3} \qquad [8]$$

The above calculations assume that the momentum distribution is symmetrical with a dependence upon radial distance. This is true for a normal incident impact.

The following table (Table 4) lists the values for P' and r_o for each of the test conditions examined in the verification study. Table 5 summarizes the results obtained from the above described calculations for total momentum. In addition, Table 5 also contains projectile momentum values along with the adjusted total momentum values which take in account only the component of the debris cloud momentum parallel to the incident projectiles motion. This is used to compute the last column of Table 5, the momentum multiplication factor.

Table 4. Verification Experiment Results for FSMMD

Experiment Designation	Maximum Debris Momentum (P')	Radial Distance (r_o)
Z-38	11.2	6.68
Z-33	4.1	9.79
Z-47	10.2	5.71
Z-51	4.5	9.38

Table 5.--Data Summary

Experiment Designation	Projectile Velocity	$P_{proj.}$ ($m_o v_o$)	P_{tot} (debris)	$P_{eff.}$ (debris)	Momentum Multiplier
Z-38 (0.1016 cm)	7.2 km/sec	260.78 kg cm/sec	518.25 kg cm/sec	395.31 kg cm/sec	1.51
Z-33 (0.2032 cm)	7.2 km/sec	260.78 kg cm/sec	407.03 kg cm/sec	260.78 kg cm/sec	1.59
Z-47 (0.1016 cm)	6.0 km/sec	217.32 kg cm/sec	344.66 kg cm/sec	477.7 kg cm/sec	2.20
Z-51 (0.2032 cm)	6.0 km/sec	217.32 kg cm/sec	410.63 kg cm/sec	310.21 kg cm/sec	1.43

It is appears from the preliminary data that the role of the bumper actually seems to increase the total effective debris cloud momentum by as much as 50%. This, however, does not violate the conservation of momentum since the primary impact also generates back scattered debris which is not measured by this technique. Similar results were obtained by the Southwest Research Institute (S_wRI) study where multiplication factors between 1.44 and 1.76 were obtained. The S_wRI study did not however, maintain the same experimental conditions as this study and therefore cannot be directly correlated. Nevertheless, the

presence of this momentum amplification factor implies that the bumper does not reduce the momentum of the debris cloud although it does result in a net energy loss from the initial impact. Therefore, any reduction in damage must be due to momentum spreading. The exact dependence and verification of this multiplying factor on impact and material parameters can not be determined from this limited amount of data but should be a logical continuation of the work now possible with the FSMMD.

V.4. Back Scattered Momentum Monitoring Device

The experiments were performed in three sets. The second and third sets of experiments repeated the conditions of the first set in test parameters, meaning the same projectiles, velocities and bumper plates. The experiments were performed in the order of the least amount of debris generation conditions performed first. This was done to improve the survivability chances of the monitoring devices.

Two different sizes of 1100 type aluminum spheres were used, .25 inch and .313 inches in diameter. The bumper plates were 12" X 16" 6061-T6 aluminum bumper plates with thicknesses varied between two conditions, .040 inch and .080 inches. The bumper plates were placed in a vice using the 16" dimension as the height. The desired projectile velocities were to be as close to 6 km/sec and 7.2 km/sec as possible. The test plan is given in Table 6.

Table 6. Hypervelocity Experiment Test Matrix

Experiment	1	2	3	4	5	6	7	8
Al Sphere .25 in .313 in	X	X	X	X	X	X	X	X
Projectile 6 km/sec 7.2 km/sec	X	X	X	X	X	X	X	X
Shield .040 in .080 in	X	X	X	X	X	X	X	X

This shows that there were to be eight different experimental conditions. The test order was not followed stringently due to time considerations involving the availability of the Light Gas Gun.

This research was aimed at the development of momentum monitoring devices for aluminum projectile-aluminum bumper hypervelocity impacts. For this particular study 6061-T6 aluminum bumper plates were used along with spherical 1100 type aluminum projectiles. The devices developed are not limited to these aluminum alloys but two shots using stainless steel projectiles impacting aluminum bumpers were made. The damage to the devices was so severe that no signals were measured. The conditions under which these momentum monitoring devices can be used require liquification or at least fragmentation of the projectile upon contact with the bumper plate.

Table 7 indicates how off-centered each of the tests were for use in determining if the momentum multiplication values truly represent certain shot parameters. Also given are the dimensions of the hole left in the aluminum bumper plates for any correlation that could be made between these dimensions and the momentum multipliers. The first analysis performed

evaluates the difference between the momentum multiplication values from the spherical approximation approach and the linear fit technique. As stated earlier the difference between shot parameters will be discussed in the conclusion. The shot sequence for the 100 series of experiments is given in Table 8. It was desired to perform all of the .25 inch projectile shots since they would cause less damage to the devices then the .313 inch.

The forward or upstream momentum multiplication values are given in Table 9 along with the backward scattered momentum multiplication values. The differences between the values can be accounted for by realizing that graphical analysis usually accounted for more area under the momentum density data curve than actually measured. The values for each of this first set of shots was suspect in that many of the critical constant values necessary for calculation actually varied.

For the first set of experiments a single front aperture shield was used. It sustained heavy damage in the innermost pendulum region. This altered the size of the aperture holes which was of great concern because the area of the hole is necessary to determine the momentum density at a particular location in the debris cloud. It was decided after the first set of shots that for the following sets of experiments new aperture shields were to be machined so that when dimensional change of the aperture holes occurred the shields could be replaced.

One set of impact blocks was used for the first three shots of the first set of experiments. The innermost pendulums, the ones located at 5 and 10 degrees, had impact blocks that were heavily deformed. Problems with the behavior of the high-density polyethylene(HDPE) pistons used in the LGG caused a delay after the first three shots. It was decided to replace

the impact blocks during this delay.

For Z101 the forward scattered device was closer to the bumper plate than six inches. The distance or angle from centerline could be adjusted to the correct dimensions but then the problem of non-normal impact to the impact blocks would have to be accounted. This would introduce more approximations that would cause a large source of error. Shot Z102 was off-centered, again causing problems with the angle at which debris strikes the surface of the impact blocks. Several of the remaining shots suffered from being off center which introduces error for both analysis techniques due to non-normal impact and angle from centerline. Test Z106 has abnormally low forward scattered momentum multiplication values. It appears that the projectile was only partially fragmented and due to not having a pendulum closer to the centerline a true representation of the debris cloud was not attained. Test Z108's forward multiplier was much larger because of the combined effect of deformed aperture holes and being off-center. As stated earlier the aperture holes had been made larger from the repeated impacts from the experiments. In the momentum density calculations the aperture sizes used for calculation were much smaller than these deformed dimensions thus the true momentum was less than the value reported.

It was decided after shot Z103 that it would be advantageous to record the dimensions of the backward scattered debris cloud. A physical record of the dimensions was to be achieved by taking photographs of the backward device's collector plate after each test. To distinguish the markings from the previous shots it was decided that painting the collector plate white would help the damage from the backward scattered debris cloud appear. It also was necessary to machine another plate so that the plates could be alternated between shots

minimizing the time required between experiments.

For the second set of experiments it was decided not only to replace the front aperture shield often but also to replace the impact blocks after every 3 shots. The impact block weights were then compared to their weights before shooting. From the measured values it was noted that none of the impact blocks gained a substantial amount of mass, less than one percent. This showed that there was no appreciable change in the moment of inertia of the hammers so that one impact block could be used for multiple shots. It was decided, though, that replacement did help ensure a certain hardness value on the collecting surface of the impact blocks.

Table 7. Bumper Plate Hole Location and Diameter

Shot Number	Y-Location from Center (in)	Hole Diameter (in)
Z101	-0.25	0.625
Z102	-0.9	0.56
Z103	-1.25	0.56
Z104	0	0.5
Z105	0	0.69
Z106	0	0.5
Z107	+0.31	0.69
Z108	-0.125	0.5
Z201	-0.5	0.63
Z202	-0.18	0.44
Z203	+0.25	0.69
Z204	+0.5	0.5
Z205	+0.25	0.69
Z206	+0.19	0.5
Z207	+0.25	0.56
Z208	+0.3	0.75
Z401	-0.25	0.63
Z402	0	0.44
Z403	+0.63	0.63
Z404	+0.5	0.5
Z406	-0.13	0.69
Z407	+0.06	0.8
Z408	-0.25	0.56

Table 8. 100 Series Shot Conditions

Shot Number	Projectile (in)	Bumper Thickness (in)	Velocity (km/s)
Z101	0.25	0.08	7.2
Z102	0.25	0.08	5.7
Z103	0.25	0.04	6.2
Z104	0.313	0.04	6.0
Z105	0.313	0.04	6.3
Z106	0.313	0.04	7.4
Z107	0.25	0.08	7.2
Z108	0.313	0.04	7.2

Table 9. 100 Series Momentum Multipliers

Shot Number	Forward Momentum Multiplier using Linear Fit	Forward Momentum Multiplier using Summation	Backward Momentum Multiplier
Z101	2.77	2.09	0.13
Z102	3.28	2.28	0.21
Z103	0.73	0.47	0.1
Z104	1.10	0.93	0.1
Z105	1.55	1.31	0.07
Z106	0.22	0.16	0.05

For the second set of experiments the conditions are given in Table 10 as follows:

Table 10. 200 Series Shot Conditions

Shot Number	Projectile (in)	Bumper Thickness (in)	Velocity (km/s)
Z201	0.25	0.08	6.0
Z202	0.25	0.04	5.9
Z203	0.25	0.08	6.9
Z204	0.25	0.04	6.4
Z205	0.313	0.08	5.9
Z206	0.313	0.04	6.1
Z207	0.313	0.04	7.1
Z208	0.313	0.08	7.2

This again shows the optimal matrix was not followed but in this series of experiments all eight conditions were tested. The momentum multipliers for the 200 series are given in Table 11. The 200 series appear to give fairly reasonable values for forward and backward momentum multipliers. Again off-centered shots caused problems with the forward momentum multiplier values being higher than may actually be occurring. From the

momentum density charts it can be seen which shots were off-centered and error that might be introduced by the curve fit. These values though did show more concurrence with the Southwest Research Institute's values between 1.4 and 1.8.

Two stainless steel shots were performed in what would have been the 300 series. As stated earlier the devices sustained so much damage from these shots no data was recorded. It was decided to do a third verification round on the aluminum shots with the new momentum monitoring devices.

Table 11. 200 Series Momentum Multipliers

Shot Number	Forward Momentum Multiplier using Linear Fit	Forward Momentum Multiplier using Summation	Backward Momentum Multiplier
Z201	2.08	1.79	0.21
Z202	1.65	0.77	0.03
Z203	1.40	1.14	0.15
Z204	1.82	1.37	0.15
Z205	1.37	0.13	0.13
Z206	3.17	1.59	0.02
Z207	1.46	1.28	0.07
Z208	1.30	1.50	0.15

The 400 series used the latest forward scattered momentum monitoring device. The conditions for the 400 series are given in Table 12 whereas the momentum multipliers for this final round of shots are given in Table 13.

Shots 403 and 404 were both off-centered to the right which causes the momentum values to be higher than may actually be the case. Shot 407 shows that the added pendulum provided a needed improvement. From the graph of the momentum density it can be seen

that there was an extremely high concentration of momentum in the center of the debris cloud. The linear fit was unable to account for the high spike in the data and cover all of the debris that was scattered to the outer pendulums as well. The summation value might be high because the aperture holes are larger than the wedge shape the surface segment of the sphere would optimally be.

Table 12. 400 Series Shot Conditions

Shot Number	Projectile (in)	Bumper Thickness (in)	Velocity (km/s)
Z401	0.25	0.08	5.7
Z402	0.25	0.04	5.7
Z403	0.25	0.08	6.7
Z404	0.313	0.04	6.0
Z406	0.313	0.08	6.1
Z407	0.313	0.08	7.0
Z408	0.313	0.04	7.0

Table 13. 400 Series Momentum Multipliers

Shot Number	Forward Momentum Multiplier using Linear Fit	Forward Momentum Multiplier using Summation	Backward Momentum Multiplier
Z401	1.56	1.48	0.18
Z402	1.86	1.09	0.08
Z403	1.82	2.21	0.18
Z404	1.73	1.79	0.04
Z406	1.11	1.55	0.24
Z407	0.67	2.04	0.04
Z408	1.24	1.31	0.02

VI. Conclusions

The following conclusions can be drawn from this investigation.

(1) The feasiblity of an in-situ measurement of debris cloud momentum distribution has been demonstrated. A device for this purpose has been developed which now provides this capability for the laboratory environment.

(2) Results from this device provide preliminary indications that a momentum multiplication factor exists with values between 1 and 2. The momentum multiplier tables show a reasonable amount of data supporting that there is a net momentum gain in the forward scattered or upstream direction. Both analysis techniques support this with their respective determined values. This forward momentum multiplication does not violate conservation of momentum because some momentum is scattered in the backward or downstream direction. This is verified not only by photographs of hypervelocity impacts but now with the backward scattered debris monitoring device used for this research.

(3) The momentum density plots show that the thicker, .08in bumper plates, caused a more widespread debris cloud. The .313in projectiles at the high end of the velocity range were barely fragmented by the .04in bumper as seen by the respective momentum density plots. Upon witnessing this partial fragmentation under the high initial momentum/thinner bumper plate condition, it was decided to locate a pendulum as close to the centerline as possible. This would verify whether or not the linear fit of the data was giving a true representation of the forward scattered momentum.

(4) The momentum multiplier data indicate that there was a high variation for each test condition. This could be because the test conditions were not exactly the same due to the light gas gun being unable to launch the projectiles at the same velocity each time. Lawrence reports that even a slight variation in shot conditions may result in varying amounts of all three phases of particles generated.[18] This could affect the momentum multiplication values as well. Another source of difference in the same parameter momentum multiplier shots can be attributed to the LGG's inability to direct the projectile's path to hit the centerline of the devices.

(5) The average values cluster around the 1.4 to 1.6 range for forward momentum amplification and 0.1 to 0.2 for the backward momentum multipliers. The backward scattered values thus indicate that there was always more debris sprayed downstream for the thicker bumper plate. This translates to a more fragmented particle which is also indicated by the wider distribution in the momentum density plots for the .08in 6061-T6 aluminum bumper shots. Net momentum above one indicates that there was more measured forward scattered momentum compared to the amount of backward scattered momentum recorded. Most of the net momentum values lie fairly close to one with notable exceptions being tests that have already been identified with large sources of error. It is felt that the deficiency of measurement primarily lied with the backward scattered monitoring device. The reason being is the inability of the device to account for contributions of off-centered shots.

VII. REFERENCES

1. Cour-Palais, B. G. and S. L. Avans, "Shielding Against Debris", June 1988, Aerospace America.

2. Long Life Design Environments, January 1989.

3. Potter, A. E., "Measuring Debris", June 1988, Aerospace America.

4. Kessler, D. J., "Current Orbital Debris Environment", Orbital Debris from Upper-Stage Breakup, Ed. by J. P. Loftus Jr., AIAA, Washington, 1989.

5. Johnson, N. L., "Evolution of the Artificial Earth Satellite Environment", Orbital Debris from Upper-Stage Breakup, Ed. by J. P. Loftus Jr., AIAA, Washington, 1989.

6. Cour-Palais, B. G. and J. L. Crews, "Hypervelocity Impact and Upper Stage Breakups", Orbital Debris from Upper-Stage Breakup, Ed. by J. P. Loftus Jr., AIAA, Washington, 1989.

7. Johnson, N. L., "Preliminary Analysis of the Fragmentation of the Spot 1 Ariane Third Stage", Orbital Debris from Upper-Stage Breakup, Ed. by J. P. Loftus Jr., AIAA, Washington, 1989.

8. Benz, F. J. et. al., "Explosive Fragmentation of Orbiting Propellant Tanks", Orbital Debris from Upper-Stage Breakup, Ed. by J. P. Loftus Jr., AIAA, Washington,1989.

9. Badhwar, G. D. et. al, "Characteristics of Satellite Breakups from Radar Cross Section and Plane-Change Angle", Orbital Debris from Upper-Stage Breakup, Ed. by J. P. Loftus Jr., AIAA, Washington, 1989.

10. Taff, L. G., "Ariane-Related Debris in Deep-Space Orbit", Orbital Debris from Upper-Stage Breakup, Ed. by J. P. Loftus Jr., AIAA, Washington, 1989.

11. Potter, A. E., K. G. Henize, and D. L. Talent, "Albedo Estimates for Debris", Orbital Debris from Upper-Stage Breakup, Ed. by J. P. Loftus Jr., AIAA, Washington, 1989.

12. Elfer, N., F. Baillif, and J. Robinson, "External Tank Space Debris Considerations", March 1992, AIAA-92-1411.

13. Baker, H. A., Space Debris: Legal and Policy Implications, Martinus Nijhoff Publishers, Boston, 1989.

14. Henize, K. G. and R. H. Rast, "Potential Spot-1 R/B-Cosmos 1680 R/B Collision", Orbital Debris from Upper-Stage Breakup, Ed. by J. P. Loftus Jr., AIAA, Washington, 1989.

15. McCormick, B., "Collision Probabilities in Geosynchronus Orbit and Techniques to Control the Environment", Orbital Debris from Upper-Stage Breakup, Ed. by J. P. Loftus Jr., AIAA, Washington, 1989.

16. Lawler, A., "Orbiting Junk May Justify Station Shield", June 1992, Space News.

17. Wirin, W. B., "Standstill on Orbital Debris Policy", June 1988, Aerospace America.

18. Loftus, J. P. E. L. Tilton, and L. P. Temple III, "Decision Time on Orbital Debris", June 1988, Aerospace America.

19. Petro, A. J. and D. L. Talent, "Removal of Orbital Debris", Orbital Debris from Upper-Stage Breakup, Ed. by J. P. Loftus Jr., AIAA, Washington, 1989.

20. Petro, A. J. and H. Ashley, "Cost Estimates for Removal of Orbital Debris", Orbital Debris from Upper-Stage Breakup, Ed. by J. P. Loftus Jr., AIAA, Washington, 1989.

21. Gray, A. A., Jr., "Current Operation Practice for the Delta Second Stage", Orbital Debris from Upper-Stage Breakup, Ed. by J. P. Loftus Jr., AIAA, Washington, 1989.

22. Hergott, R., "Ariane Third Stage: Current Operational Practice and Modifications Expected", Orbital Debris from Upper-Stage Breakup, Ed. by J. P. Loftus Jr., AIAA, Washington, 1989.

23. Groesbeck, W., "Centaur Upper Stage", Orbital Debris from Upper-Stage Breakup, Ed. by J. P. Loftus Jr., AIAA, Washington, 1989.

24. Noda, K., "Safing of H-1 Second Stage After Spacecraft Separation", Orbital Debris from Upper-Stage Breakup, Ed. by J. P. Loftus Jr., AIAA, Washington, 1989.

26. Meteoroid/Debris Shielding Development Test (D-6) Test Plan, Boeing, October 1990.

27. Whipple, F., "Meteroites and Space Travel", Astronomical Journal, No. 1161, 1947.

28. Schonberg, W. and R. Taylor, "Design of a Secondary Debris Containment Shield for Large Space Structures", April 1989, AIAA-89-1412.

29. Christensen, E. L., J. L. Hyde, and G. Snell, "Spacecraft Survivability in the Meteroid and Debris Environment", March 1992, AIAA-92-1409.

30. Cour-Palais, B.G., "Space Vehicle Meteroid Shielding Design", April 1979, The Comet Halley Micrometeoroid Hazard Workshop Proceedings ESA-SP153.

31. Christiansen, E. L., "Performance Equations for Advanced Orbital Debris Shields", March 1992, AIAA-92-1462.

32. Cour-Palais, B. G., "Hypervelocity Impact Investigations and Meteoroid Shielding Experience Related to Apollo and Skylab", July 1982, Orbital Debris NASA Conference Publication 2360.

33. Swift, H. F., Hopkins, A. K., "Effects of Bumper Material Properties on the Operation of Spaced Meteroid Shields", January 1970, J. Spacecraft.

34. Zwiener, J., Mount, A.,"An Enhanced Whipple Bumper System: Impact Resistance of Composite Materials", March 1992, AIAA.

35. Swift, H. F., Carson, J.M.,"Ballistic Limits of 6061-T6 Aluminum Bumper Systems" October 1967, Technical Report AFML-TR-67-324.

36. Cour-Palais, B. G., "Meteroid Protection by Multi-Walled Structures", May 1969, AIAA-69-372.

37. Cour-Palais, B. G. and J. L. Crews, "A Multi-Shock Concept for Space Craft Shielding", 1990, Int. J. of Impact Engineering.

38. Walker, E. J., and Schonberg, W. P., "Simultated Orbital Debris Impact of Multi-Wall Composite Structures", March 1992, AIAA-92-1628.

39. Schonberg, W. P., and R. A. Taylor, "Oblique Hypervelocity Impact Response of Dual-Sheet Structures", January 1989, NASA-TM-100358.

40. Anderson, E. C., "An Overview of the Theory of Hydrocodes", 1987, Int. J. of

Impact Engineering.

41. Smith, R. H., "Investigation of Crater Growth and Ejecta Cloud Resulting from Hypervelocity Impact of Aluminum Spheres on Thick Aluminum Targets", June 1968, AFML-TR-68-175.

42. Kinard, W. H., et. al., "Particles in Space - LDEF Helps to Understand a Complex Environment", LDEF Spaceflight Environmental Effects Newsletter, June 1993, Vol IV, No. 3.

43. Ang, J. A., et. al., "Pulsed Holography for Hypervelocity Impact Diagnostics", 1991, SAND-91-2871C.

44. Mullin, Scott A., et. al., "Dissimilar Material Velocity Scaling for Hypervelocity Impact", Hypervelocity Impact Symposium, 1989.

45. Denardo, B. P., and C. R. Nysmith, "Momentum Transfer and Cratering Phenomena Associated with the Impact of Aluminum Spheres into Thick Aluminum Targets at Velocities to 24,000 Feet Per Second", NASA, 1964.

46. Nysmith, C.R., and B. P. Denardo, "Experimental Investigation of the Momentum Transfer Associated with Impact into Thin Aluminum Targets", NASA,TND-5492, 1969. OK

47. Trans-Science Corporation Hypervelocity Penetration Mechanics Research Proposal, Submitted to NASA/DARPA, 1990.

48. Smith, H.F., and R.F. Prater, "Simulation of High Velocity Impacts on Thin Targets", May 1968, AFML-TR-68-88.

49. Abbot, R. D., and M. D. Bjorkman, "Momentum Transfer in One-Dimensional

Impact of Space Plates, Boeing Co., 1991.

50. Berggren, R. E. and R. M. Reynolds, "The Light Gas Gun Model Launcher", Ballistic Range Technology, Ed. by Canning, T. N., A. Seiff, and C.S. James, August 1970.

51. Balllistic Range Tech., Camera section

52. Piekutowski, Andrew J., "Structural Damage Prediction and Analysis for Hypervelocity Impacts", May 1991

53. Taylor, R. A.," A Space Debris Simulation Facility for Spacecraft Materials Evaluation", SAMPE Quaterly, Vol. 18, No. 2, 1987.

54. Standard Operating and Safety Procedure for Micrometeoroid/Space Debris Impact Test Facility, NASA MSFC.

55. Zee, R. H., "A Dynamic Study of Fragmentation and Energy Loss During High Velocity Impact", NASA, 1990.

56. LeMaster, P. S., A. Mount, and R. H. Zee," Momentum Distribution in Debris Cloud During Hypervelocity Impact", AIAA, 1992.